

^{85}Rb , ^{87}Rb , and ^{17}O nuclear-quadrupole-resonance study of $\text{Rb}(\text{H}_{1-x}\text{D}_x)_2\text{PO}_4$

J. Seliger, V. Žagar, and R. Blinc

"J. Stefan" Institute, E. Kardelj University of Ljubljana, Ljubljana, Yugoslavia

V. H. Schmidt

Department of Physics, Montana State University, Bozeman, Montana

(Received 19 March 1990)

The ^{85}Rb , ^{87}Rb , and ^{17}O nuclear-quadrupole-resonance frequencies and line shapes have been measured in RbH_2PO_4 and in $\text{Rb}(\text{H}_{1-x}\text{D}_x)_2\text{PO}_4$ ($x=0.5, 0.7$) with the nuclear-quadrupole double-resonance technique. The results show that in the paraelectric phase the Rb^+ ions move in a single-site potential, whereas the protons are dynamically disordered between two sites in the $\text{O}-\text{H}\cdots\text{O}$ hydrogen bonds. The ferroelectric phase transition in RbH_2PO_4 is associated with the freezing out of the proton motion in the $\text{O}-\text{H}\cdots\text{O}$ hydrogen bonds that induces a shift of the Rb^+ ions along the ferroelectric axis. In the partially deuterated compounds the $\text{O}-\text{H}\cdots\text{O}$ hydrogen bonds are practically identical to the ones in pure RbH_2PO_4 and are thus only weakly influenced by the surrounding $\text{O}-\text{D}\cdots\text{O}$ bonds. The $\text{O}-\text{D}\cdots\text{O}$ bonds are, however, significantly more asymmetric and presumably longer than the $\text{O}-\text{H}\cdots\text{O}$ bonds.

I. INTRODUCTION

Rubidium dihydrogen phosphate RbH_2PO_4 , is a hydrogen-bonded ferroelectric that undergoes the ferroelectric phase transition at $T_c = -126^\circ\text{C}$.¹ Its structure is isomorphous to that of KH_2PO_4 in both the tetragonal paraelectric and the orthorhombic ferroelectric phase.² The PO_4 groups are linked by the $\text{O}-\text{H}\cdots\text{O}$ hydrogen bonds in which the protons are above T_c disordered between the two equivalent equilibrium sites. The ferroelectric phase transition is associated with the freezing out of the proton motion and the displacement of heavy ions.

Remarkable changes occur on deuteration. Both $\text{K}(\text{H}_{1-x}\text{D}_x)_2\text{PO}_4$ and $\text{Rb}(\text{H}_{1-x}\text{D}_x)_2\text{PO}_4$ exhibit a monoclinic phase at room temperature and at high-deuteration levels and the ferroelectric-paraelectric transition temperature increases markedly with deuteration. The neutron³ and the x-ray⁴ diffraction studies showed that the $\text{O}-\text{D}\cdots\text{O}$ bond is slightly longer but considerably more asymmetric than the $\text{O}-\text{H}\cdots\text{O}$ bond.

Nuclear quadrupole resonance (NQR) has proved to represent a sensitive tool for the study of even small structural changes in the crystals. Therefore we decided to measure the ^{85}Rb , ^{87}Rb , and ^{17}O NQR frequencies in RbH_2PO_4 and in $\text{Rb}(\text{H}_{1-x}\text{D}_x)_2\text{PO}_4$ in order to clarify the role of the $\text{O}-\text{D}\cdots\text{O}$ hydrogen bonds in partially deuterated systems.

II. EXPERIMENTAL

^{87}Rb has a spin $I = \frac{3}{2}$ and thus in zero magnetic field two doubly degenerated energy levels with the corresponding NQR frequency

$$\nu_Q = \frac{eQV_{ZZ}}{2h} [(1 + \eta^2/3)]^{1/2}. \quad (1)$$

Here eQ is the nuclear quadrupole moment, V_{ZZ} is the largest principal value of the electric-field-gradient (EFG) tensor, $V_{ij} = \partial^2 V / \partial x_i \partial x_j$, at the nuclear site and the asymmetry parameter η is the difference of the two smaller principal values of the EFG tensor $V_{XX} - V_{YY}$, $|V_{XX}| \leq |V_{YY}| \leq |V_{ZZ}|$, divided by V_{ZZ} . The quadrupole coupling constant eQV_{ZZ}/h and the asymmetry parameter can not be separately determined from the NQR frequency.

^{85}Rb has a spin $I = \frac{5}{2}$ and thus in zero magnetic field three doubly degenerated quadrupole energy levels. Their energies E are obtained from the secular equation

$$x^3 - 7(3 + \eta^2)x - 20(1 - \eta^2) = 0, \quad (2)$$

where the energy $E = xA$ and $A = eQV_{ZZ}/40$. For each chemically inequivalent rubidium site we thus obtain three ^{85}Rb NQR frequencies $\nu_{(1/2)-(3/2)} \leq \nu_{(3/2)-(5/2)} < \nu_{(1/2)-(5/2)} = \nu_{(1/2)-(3/2)} + \nu_{(3/2)-(5/2)}$. The asymmetry parameter η is calculated from the ratio $\nu_{(1/2)-(3/2)} / \nu_{(3/2)-(5/2)}$. When η is known the quadrupole coupling constant can be calculated from any NQR frequency.

^{17}O has a spin $I = \frac{5}{2}$ and the NQR frequencies, the quadrupole coupling constant, and the asymmetry parameter η can be obtained in the same way as for ^{85}Rb . In the $\text{O}-\text{H}$ bonds the strong proton-oxygen magnetic dipolar interaction removes the degeneracy of the ^{17}O energy levels. Each energy level splits into a quartet and the NQR lines become broad and structured. From the widths and structures of the ^{17}O NQR lines the $\text{O}-\text{H}$

distance as well as the orientation of the O—H bond in the eigenframe of the EFG tensor at the oxygen site can be determined.^{5,6}

The ⁸⁵Rb, ⁸⁷Rb, and ¹⁷O NQR frequencies have been measured with a nuclear-quadrupole double-resonance (NQDR) technique based on magnetic-field cycling between a high-static and zero magnetic field and phase modulated rf irradiation in zero magnetic field.^{7,8} The dipolar structures of the ¹⁷O NQR lines have been measured with a nuclear-quadrupole double-resonance technique based on magnetic-field cycling and two-frequency irradiation.⁵

III. RESULTS AND DISCUSSION

A. RbH₂PO₄

The temperature dependence of the ⁸⁵Rb and ⁸⁷Rb NQR frequencies is shown in Fig. 1. The corresponding quadrupole coupling constants and the asymmetry parameter are shown in Fig. 2. Above the phase transition the ⁸⁵Rb quadrupole coupling constant is 19.97 MHz, the ⁸⁷Rb quadrupole coupling constant is 9.68 MHz, and the asymmetry parameter η is zero. The ratio of the two rubidium quadrupole coupling constants $19.97 \text{ MHz} / 9.68 \text{ MHz} = 2.063$ is equal to the ratio of two rubidium nuclear quadrupole moments $Q(^{85}\text{Rb})/Q(^{87}\text{Rb})$. Below the phase transition the rubidium quadrupole coupling con-

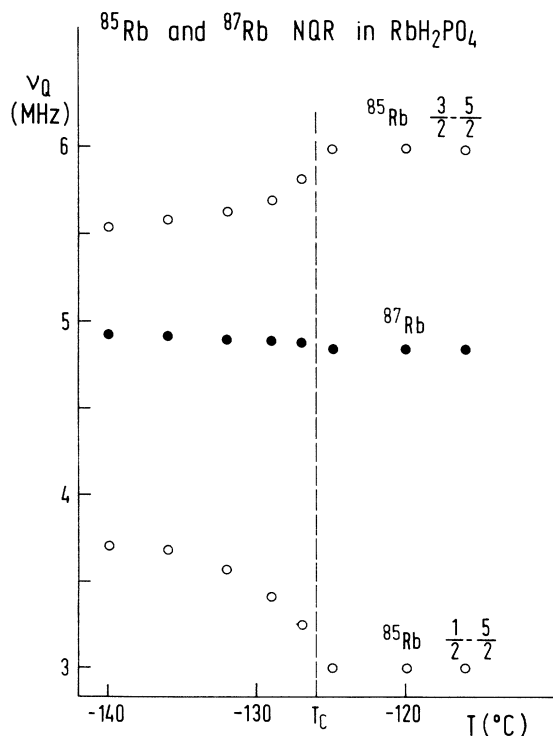


FIG. 1. Temperature dependence of the ⁸⁵Rb and ⁸⁷Rb NQR frequencies in RbH₂PO₄.

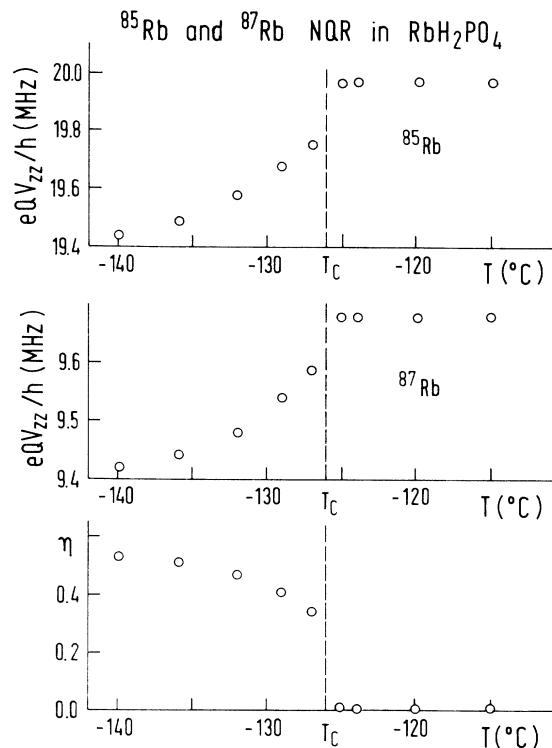


FIG. 2. Temperature dependences of the ⁸⁵Rb quadrupole coupling constant, ⁸⁷Rb quadrupole coupling constant, and of the asymmetry parameter η of the EFG tensor at the rubidium sites in RbH₂PO₄.

stants slightly decrease and the asymmetry parameter η strongly increases with decreasing temperature. Thus at -140°C the ⁸⁵Rb quadrupole coupling constant is 19.44 MHz and the asymmetry parameter η is 0.53. The present NQR data agree with the previously published data⁹ obtained by the quadrupole perturbed NMR technique. However, the resolution of the presently used nuclear-quadrupole double-resonance technique is much higher than the resolution of the quadrupole perturbed NMR technique.

There are two possible models of the ferroelectric phase transition in the KH₂PO₄ type crystals. According to the first of these two models the Rb⁺ ions are in the paraelectric phase dynamically disordered between two equivalent equilibrium positions similarly as the O—H···O protons. According to the second model only the O—H···O protons (or deuterons) are disordered between two equilibrium sites, whereas the Rb⁺ ions move in an anharmonic single-site potential above T_c .

In the two site Rb⁺ order-disorder model we assume that the rubidium ions are in the paraelectric phase disordered between the two equivalent equilibrium positions along the $\bar{4}$ axis that is also the Z-principle axis of the electric-field gradient tensor. One of these position is at $-z$ and another at $+z$ with respect to the average rubidium position. The two ERG tensors $V(z)$ and $V(-z)$ have, according to the site symmetry of rubidium, the following forms:

$$\begin{aligned}
 V(z) &= \begin{bmatrix} V_{XX} & 0 & 0 \\ 0 & V_{YY} & 0 \\ 0 & 0 & V_{ZZ} \end{bmatrix}, \\
 V(-z) &= \begin{bmatrix} V_{YY} & 0 & 0 \\ 0 & V_{XX} & 0 \\ 0 & 0 & V_{ZZ} \end{bmatrix}.
 \end{aligned} \tag{3}$$

Here the Z axis is the crystallographic c axis, while the X and Y axes are lying in the a - b plane. In the paraelectric

$$\begin{aligned}
 \langle V \rangle &= \frac{1+S}{2} V(z) + \frac{1-S}{2} V(-z) \\
 &= \begin{bmatrix} [-V_{ZZ} + S(V_{XX} - V_{YY})]/2 & 0 & 0 \\ 0 & [-V_{ZZ} - S(V_{XX} - V_{YY})]/2 & 0 \\ 0 & 0 & V_{ZZ} \end{bmatrix}.
 \end{aligned} \tag{5}$$

Here S is the order parameter. Thus the quadrupole coupling constant eQV_{ZZ} remains the same as in the paraelectric phase, whereas the asymmetry parameter η ,

$$\eta = (\langle V \rangle_{XX} - \langle V \rangle_{YY}) / \langle V \rangle_{ZZ} = S(V_{XX} - V_{YY}) / V_{ZZ}, \tag{6}$$

is proportional to the order parameter. By comparing the experimentally determined values of η with the temperature dependence of the spontaneous polarization P_s (Ref. 10) we found that η is indeed proportional to the spontaneous polarization and thus to the order parameter. The limiting value of η in case of complete ordering ($S=1$) is then obtained from the temperature dependence of P_s ; It is equal to 0.59. The quadrupole coupling constant is not temperature independent in the ferroelectric phase as expected from expression (5) but it slightly decreases with decreasing temperature. Presumably the separation of $2z$ of the two equilibrium positions slightly increases with increasing order parameter. Nevertheless, it is hard to believe that a displacement Δz of the equilibrium site would cause a change of the quadrupole coupling constant that is proportional to the square of the order parameter.

Another possible explanation of the NQR data is the proton order-disorder model with a single-site Rb potential. Here we assume that in the paraelectric phase a rubidium ion stays at rest in its paraelectric position and displaces from the paraelectric position below T_c . We assume that the displacement z of a rubidium ion induced by the ordering of protons is proportional to the order parameter. The elements of the EFG tensor can be expanded in power series in the displacement z . Owing to the symmetry of the rubidium site the following relations hold [expressions (3)]:

$$\begin{aligned}
 V_{ZZ}(-z) &= V_{ZZ}(z), \\
 V_{XX}(-z) &= V_{YY}(z),
 \end{aligned} \tag{7}$$

phase the time averaged EFG tensor $\langle V \rangle$ is

$$\langle V \rangle = \frac{1}{2} [V(-z) + V(z)] = \begin{bmatrix} -V_{ZZ}/2 & 0 & 0 \\ 0 & -V_{ZZ}/2 & 0 \\ 0 & 0 & V_{ZZ} \end{bmatrix}. \tag{4}$$

Thus the asymmetry parameter η is zero what agrees with the NQR data. In the ferroelectric phase the two equilibrium positions are no more equivalent and the time-averaged EFG tensor $\langle V \rangle$ is

and from them we obtain

$$\begin{aligned}
 V_{XX}(z) &= -V_{ZZ}/2 + az + bz^2 + \dots, \\
 V_{YY}(z) &= -V_{ZZ}/2 - az + bz^2 - \dots, \\
 V_{ZZ}(z) &= V_{ZZ} - 2bz^2 + \dots.
 \end{aligned} \tag{8}$$

Here V_{ZZ} is the largest principal value of the EFG tensor at the rubidium site in the paraelectric phase. To the lowest order in z , the asymmetry parameter η ,

$$\eta = 2az / V_{ZZ}, \tag{9}$$

is proportional to z and thus to the order parameter, while the shift of the quadrupole coupling constant,

$$(eQ/h)[V_{ZZ}(T > T_c) - V_{ZZ}(T < T_c)] = 2bz^2, \tag{10}$$

is proportional to the square of the order parameter in agreement with the NQR data. The NQR data thus seem to support the proton order-disorder model with a single-site potential for the Rb^+ ions. Thus we believe that above T_c each proton is disordered between two equivalent equilibrium sites in an $\text{O}-\text{H} \cdots \text{O}$ hydrogen bond, while the rubidium ions are at rest. Below T_c protons order and the rubidium ions displace from their paraelectric positions.

The temperature dependence of the ¹⁷O NQR frequencies in RbH_2PO_4 is shown in Fig. 3 and the corresponding quadrupole coupling constants and asymmetry parameters are shown in Fig. 4. All the oxygen sites are chemically equivalent above T_c , whereas two chemically inequivalent oxygen sites are observed below T_c in agreement with the proposed model of proton ordering in the $\text{O}-\text{H} \cdots \text{O}$ hydrogen bonds. In view of the dipolar coupling with protons the ¹⁷O NQR lines corresponding to the "close" (O-H) sites are broad and the ¹⁷O NQR lines corresponding to the "distant" (O \cdots H) sites are nar-

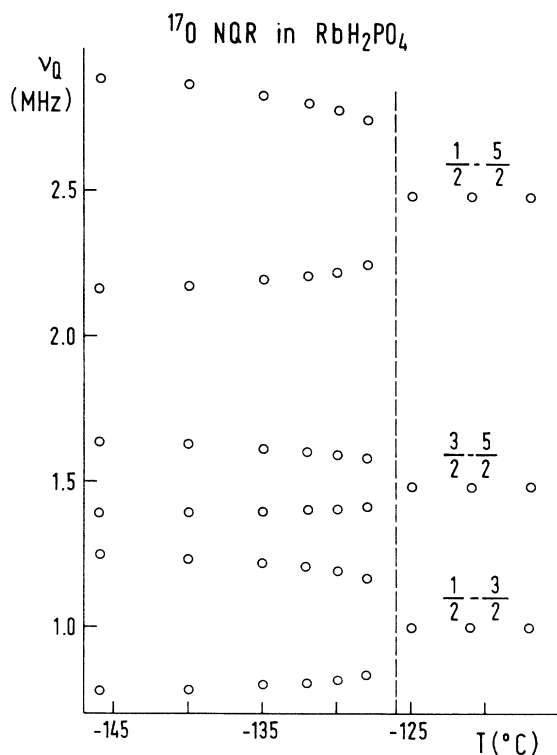


FIG. 3. Temperature dependence of the ^{17}O NQR frequencies in RbH_2PO_4 .

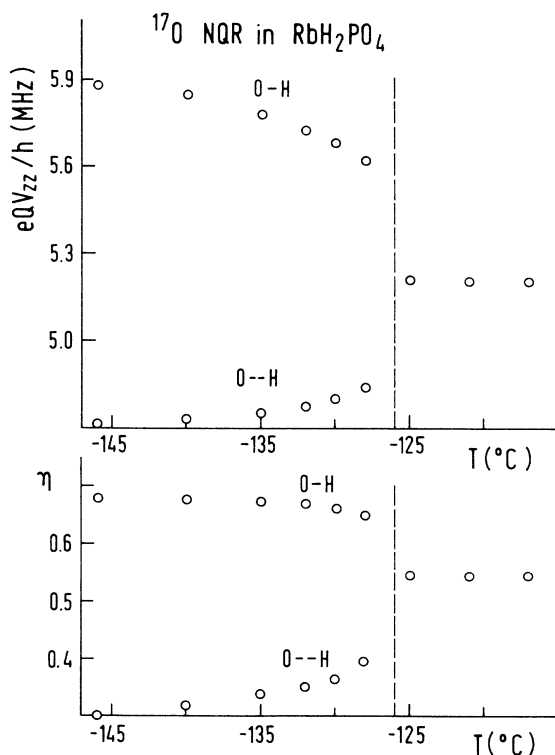


FIG. 4. Temperature dependence of the ^{17}O quadrupole coupling constants and asymmetry parameters in RbH_2PO_4 .

row. Below T_c the average value of the two intermediate principal values V_{YY} multiplied by eQ/h : $eQ[V_{YY}(\text{O-H}) + V_{YY}(\text{O}\cdots\text{H})]/2h$ is temperature independent and is equal to $eQV_{YY}(T > T_c)/h = 4.01$ MHz. The difference $eQV_{YY}(\text{O-H})/h - eQV_{YY}(\text{O}\cdots\text{H})/h$ is within the experimental resolution proportional to the order parameter S and reaches the value (2.05 ± 0.04) MHz at $S = 1$. From the structure of a hydrogen-bonded PO_4 group we may expect that one of the principal axes of the EFG tensor at the O-H site as well as one of the principal axes of the EFG tensor at the $\text{O}\cdots\text{H}$ site point approximately perpendicular to the P-O-H plane and are thus perpendicular to the O-H bond. The NQR data suggest this to be in both cases the Y axes, similarly as in KH_2PO_4 .¹¹ Thus the intermediate principal value $\langle V \rangle_{YY}$ of the time averaged EFG tensor $\langle V \rangle$ is for the O-H site

$$\langle V(\text{O-H}) \rangle_{YY} = \frac{1+S}{2} V_{YY}(\text{O-H}) + \frac{1-S}{2} V_{YY}(\text{O}\cdots\text{H}) \quad (11)$$

and for the $\text{O}\cdots\text{H}$ site

$$\langle V(\text{O}\cdots\text{H}) \rangle_{YY} = \frac{1-S}{2} V_{YY}(\text{O-H}) + \frac{1+S}{2} V_{YY}(\text{O}\cdots\text{H}) \quad (12)$$

The average value

$$\frac{1}{2} [\langle V(\text{O-H}) \rangle_{YY} + \langle V(\text{O}\cdots\text{H}) \rangle_{YY}], \quad (13)$$

$$\begin{aligned} \frac{1}{2} [\langle V(\text{O-H}) \rangle_{YY} + \langle V(\text{O}\cdots\text{H}) \rangle_{YY}] \\ = \frac{1}{2} [V_{YY}(\text{O-H}) + V_{YY}(\text{O}\cdots\text{H})], \end{aligned}$$

is constant while the difference $\langle V(\text{O-H}) \rangle_{YY} - \langle V(\text{O}\cdots\text{H}) \rangle_{YY}$,

$$\begin{aligned} \langle V(\text{O-H}) \rangle_{YY} - \langle V(\text{O}\cdots\text{H}) \rangle_{YY} \\ = S[V_{YY}(\text{O-H}) - V_{YY}(\text{O}\cdots\text{H})], \quad (14) \end{aligned}$$

is proportional to the order parameter S and measures the asymmetry of the $\text{O-H}\cdots\text{O}$ hydrogen bond. In case of complete ordering ($S = 1$) we may also expect that the asymmetry of the $\text{O-H}\cdots\text{O}$ bond as well as the difference $V_{YY}(\text{O-H}) - V_{YY}(\text{O}\cdots\text{H})$ increases with increasing O-O distance.

In order to test the above assumption and to find the O-H distance we have measured the dipolar structures of the three ^{17}O -H NQR lines at -135°C . The experimental results are shown in Fig. 5. The O-H distance as deduced from the dipolar structures of the ^{17}O NQR lines is (0.1075 ± 0.001) nm and the O-H bond lies in the X - Z plane of the EFG tensor forming an angle of $36^\circ \pm 3^\circ$ with the Z axis. Thus the Y axis is indeed perpendicular to the O-H bond. The O-H distance seems to be longer than 0.106 nm as obtained by neutron diffraction.² However, at -135°C the protons are not yet completely ordered

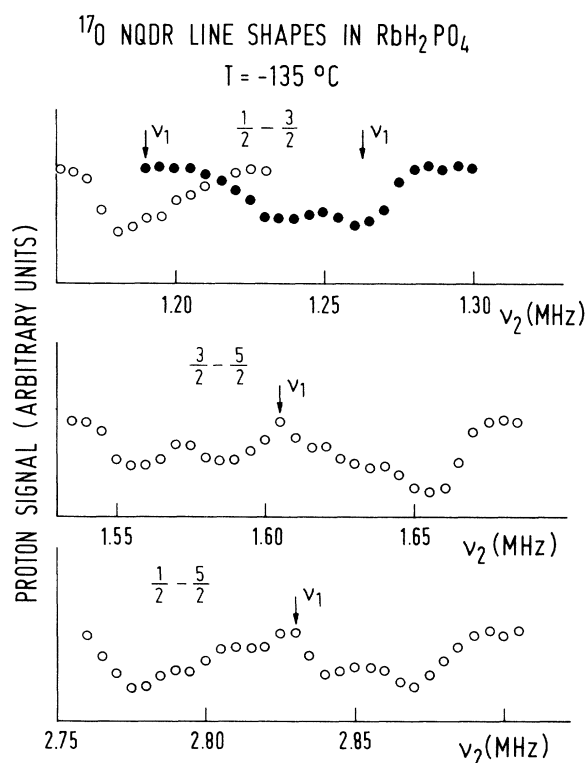


FIG. 5. Dipolar structures of the ^{17}O -H NQR lines in RbH_2PO_4 at -135°C as obtained by the two-frequency irradiation. The fixed irradiation frequencies (ν_1) are indicated by the arrows.

and the proton-oxygen dipolar coupling depends on a time averaged O-H distance R defined as

$$R^{-3} = \frac{1+S}{2} R(\text{O-H})^{-3} + \frac{1-S}{2} R(\text{O}\cdots\text{H})^{-3}. \quad (15)$$

Here S is the order parameter that is at -135°C equal to 0.85, $R(\text{O-H})$ is the short O-H distance and $R(\text{O}\cdots\text{H})$ is the long O \cdots H distance within an O—H \cdots O bond. By inserting $R = 0.1075$ nm, $S = 0.85$, and $R(\text{O-O}) = R(\text{O-H}) + R(\text{O}\cdots\text{H}) = 0.251$ nm into Eq. (11) we obtain $R(\text{O-H}) = (0.106 \pm 0.001)$ nm and $R(\text{O}\cdots\text{H}) = 0.145$ nm in good agreement with the neutron-diffraction results.

B. $\text{Rb}(\text{H}_{1-x}\text{D}_x)_2\text{PO}_4$

The ^{17}O NQR frequencies have been measured in $\text{Rb}(\text{H}_{0.5}\text{D}_{0.5})_2\text{PO}_4$ and in $\text{Rb}(\text{H}_{0.3}\text{D}_{0.7})_2\text{PO}_4$. In both substances the ^{17}O NQR frequencies are equal within the experimental resolution and they are below -130°C temperature independent. For the O-H site the two lower ^{17}O NQR frequencies are $\nu_{(1/2)-(3/2)} = 1280$ kHz and $\nu_{(3/2)-(5/2)} = 1665$ kHz, the quadrupole coupling constant eQV_{ZZ}/h is 5980 kHz, and the asymmetry parameter η is 0.69. For the O \cdots H site the two lower ^{17}O NQR frequencies are $\nu_{(1/2)-(3/2)} = 755$ kHz and $\nu_{(3/2)-(5/2)} = 1388$ kHz, the quadrupole coupling constant is 4690 kHz, and the asymmetry parameter η is 0.26. The widths of the

^{17}O NQR lines are nearly the same as in RbH_2PO_4 . This demonstrates that the distributions of the ^{17}O NQR frequencies in the O—H \cdots O bonds due to the random distribution of deuterons are rather narrow. Nevertheless, the dipolar structures of the ^{17}O NQR lines are much better resolved in RbH_2PO_4 than in the partially deuterated compounds although the proton-proton dipolar interactions that partially smear out the dipolar structures decrease with the increasing deuterium concentration. The average $eQ[V_{YY}(\text{O-H}) + V_{YY}(\text{O}\cdots\text{H})]/2h$ of the intermediate principal values of the EFG tensors at the O-H site and at the O \cdots H site is the same as in RbH_2PO_4 , while their difference $eQ[V_{YY}(\text{O-H}) - V_{YY}(\text{O}\cdots\text{H})]/h$, which measures the asymmetry of the O—H \cdots O hydrogen bond is equal to (2.10 ± 0.04) MHz, which is within the limits of experimental resolution equal to the value obtained in RbH_2PO_4 at $S = 1$. Since the asymmetry of the O—H \cdots O hydrogen bond is expected to increase with increasing O-O distance we may conclude that the O—H \cdots O bonds in $\text{Rb}(\text{H}_{1-x}\text{D}_x)_2\text{PO}_4$ are not very much affected by the surrounding O—D \cdots O bonds and that they are of nearly the same length as in RbH_2PO_4 .

The ^{17}O nuclei at the O-D sites and at the O \cdots D sites are rather far from the closest protons and have not been observed.

A more pronounced difference between RbH_2PO_4 and $\text{Rb}(\text{H}_{1-x}\text{D}_x)_2\text{PO}_4$ can be seen from the ^{85}Rb NQR spectra. The three ^{85}Rb NQR line shapes in $\text{Rb}(\text{H}_{0.5}\text{D}_{0.5})_2\text{PO}_4$ at $T = -140^\circ\text{C}$ are shown in Fig. 6. The ^{85}Rb NQR line shapes in RbH_2PO_4 at $T = -140^\circ\text{C}$

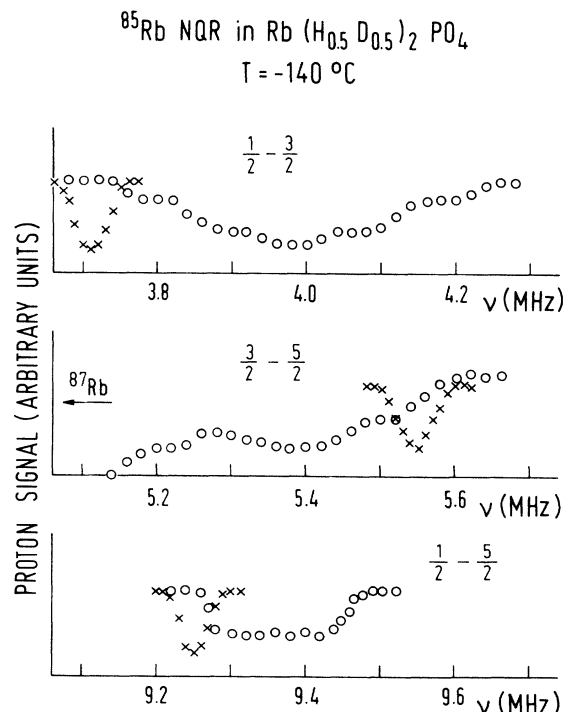


FIG. 6. ^{85}Rb NQR line shapes in $\text{Rb}(\text{H}_{0.5}\text{D}_{0.5})_2\text{PO}_4$ (open circles) and in RbH_2PO_4 (crosses) at -140°C .

are shown for comparison. In the partially deuterated compound the ^{85}Rb NQR lines are structured and markedly broader than in the nondeuterated compound. In the partially deuterated compound we in fact observe the distributions of the ^{85}Rb NQR frequencies that depend on the distribution of deuterons and protons in the hydrogen bonds surrounding the rubidium ions. The $\frac{1}{2}-\frac{3}{2}$ transition frequencies extend from 3.8 MHz, which is approximately the $\frac{1}{2}-\frac{3}{2}$ transition frequency in RbH_2PO_4 at $S=1$ to 4.2 MHz. The $\frac{3}{2}-\frac{5}{2}$ transition frequencies extend from 5.2 to 5.5 MHz, which is approximately the $\frac{3}{2}-\frac{5}{2}$ transition frequency in RbH_2PO_4 at $S=1$. The $\frac{1}{2}-\frac{5}{2}$ transition frequencies extend from 9.3 to 9.4 MHz. The quadrupole coupling constants and asymmetry parameters range from $eQV_{ZZ}/h=19.1$ MHz, $\eta=0.60$ to $eQV_{ZZ}/h=18.9$ MHz, $\eta=0.75$. The distribution limits $eQV_{ZZ}/h=19.1$ MHz and $\eta=0.60$ are equal to the quadrupole coupling constant and the asymmetry parameter in RbH_2PO_4 extrapolated to $S=1$. This agrees with the conclusion, based on the ^{17}O NQR, that the asymmetry of the $\text{O}-\text{H}\cdots\text{O}$ hydrogen bonds does not significantly change in partially deuterated compounds. The other limits: $eQV_{ZZ}/h=18.9$ MHz, $\eta=0.75$ may be assigned to the rubidium sites surrounded by deuterons (RbD_2PO_4). Since the asymmetry parameter is proportional to the spontaneous polarization in RbH_2PO_4 , or to the local polarization in $\text{Rb}(\text{H}_{1-x}\text{D}_x)_2\text{PO}_4$, it is clear that the $\text{O}-\text{D}\cdots\text{O}$ bonds in the mixed crystals are indeed more asymmetric and longer than the $\text{O}-\text{H}\cdots\text{O}$ bonds as already concluded from the neutron-diffraction data.³ Moreover, we may on the basis of the NQR data conclude that the spontaneous polarization in RbH_2PO_4 exceeds the spontaneous polarization in RbD_2PO_4 by approximately 25%. A similar difference between the spontaneous polarization in KD_2PO_4 and in KH_2PO_4 has been observed by Chabin and Gilletta.¹²

The structures of the NQR frequency distributions are presumably due to the rubidium interactions with the closest oxygens that many participate in the $\text{O}-\text{H}\cdots\text{O}$ or in the $\text{O}-\text{D}\cdots\text{O}$ hydrogen bonds.

In $\text{Rb}(\text{H}_{0.3}\text{D}_{0.7})_2\text{PO}_4$ the ^{85}Rb NQR frequencies are distributed in the same frequency ranges as in $\text{Rb}(\text{H}_{0.5}\text{D}_{0.5})_2\text{PO}_4$, with the only difference that the frequency distributions become asymmetric: stronger at the RbD_2PO_4 side and weaker at the RbH_2PO_4 side in agreement with the above assumptions.

IV. CONCLUSIONS

The ^{17}O NQR measurements in RbH_2PO_4 show that the ferroelectric phase transition is indeed associated with the ordering of protons in the $\text{O}-\text{H}\cdots\text{O}$ hydrogen bonds. The difference of the two intermediate principal values of the EFG tensors at the O-H site and at the $\text{O}\cdots\text{H}$ site: $V_{YY}(\text{O}-\text{H})-V_{YY}(\text{O}\cdots\text{H})$ is proportional to the order parameter and also to the spontaneous polarization. The O-H distance as deduced from the dipolar structures of the ^{17}O NQR lines (0.106 ± 0.001) nm, agrees with the value obtained by neutron diffraction.

The ^{85}Rb NQR results have been analyzed with two models of the ferroelectric phase transition: (i) with a model in which the rubidium ions are in the paraelectric phase dynamically disordered between two equivalent equilibrium positions, similarly as protons, and (ii) with a model in which the rubidium ions are in the paraelectric phase moving in an anharmonic single-site potential and displace from their paraelectric positions along the ferroelectric axis below T_c . The NQR data seem to support the second model in which the asymmetry parameter η is proportional to the displacement of a rubidium ion.

The ^{17}O NQR data in $\text{Rb}(\text{H}_{1-x}\text{D}_x)_2\text{PO}_4$ show only narrow distributions of the NQR frequencies and the difference $V_{YY}(\text{O}-\text{H})-V_{YY}(\text{O}\cdots\text{H})$ is nearly the same as in RbH_2PO_4 in the case of the complete proton ordering. Thus the asymmetry of the $\text{O}-\text{H}\cdots\text{O}$ bonds is in partially deuterated samples nearly the same as in RbH_2PO_4 .

Rather broad distributions of the ^{85}Rb quadrupole coupling constants and of the asymmetry parameters have been observed in the partially deuterated samples, ranging from the values found in RbH_2PO_4 to the values assigned to RbD_2PO_4 . The asymmetry parameter η of the EFG tensor at the rubidium site is in RbD_2PO_4 , by approximately 25%, larger than in RbH_2PO_4 , demonstrating that the displacement of a rubidium ion from its paraelectric position is in RbD_2PO_4 , by approximately 25%, larger than in RbH_2PO_4 . Thus the $\text{O}-\text{D}\cdots\text{O}$ bonds are indeed longer and more asymmetric than the $\text{O}-\text{H}\cdots\text{O}$ bonds. The electric dipole moment associated with an $\text{O}-\text{D}\cdots\text{O}$ bond is, by approximately 25% larger than the electric dipole moment associated with an $\text{O}-\text{H}\cdots\text{O}$ bond. This microscopic determination of the isotope effect in the electric dipole moments agrees with the results of the macroscopic measurements of the spontaneous polarization.

¹P. Bartschi, B. Matthias, W. Merz, and P. Scherrer, *Helv. Phys. Acta* **18**, 240 (1945).

²N. S. J. Kennedy and R. J. Nelmes, *J. Phys. C* **13**, 4841 (1980).

³J. E. Tibballs, W.-L. Zhong, and R. J. Nelmes, *J. Phys. C* **15**, 4431 (1982).

⁴A. A. Rusakov, L. A. Muradyan, and D. M. Kheiker, *Kristallografiya* **24**, 247 (1979) [*Sov. Phys.—Crystallogr.* **24**, 139 (1979)].

⁵S. G. P. Brosnan and D. T. Edmonds, *J. Magn. Res.* **38**, 47 (1980).

⁶J. Seliger, V. Žagar, R. Blinc, and A. Novak, *J. Chem. Phys.* **84**, 5857 (1986).

⁷R. E. Slusher and E. L. Hahn, *Phys. Rev.* **166**, 332 (1968).

⁸S. R. Hartmann and E. L. Hahn, *Phys. Rev.* **128**, 2042 (1962).

⁹R. Blinc, D. E. O'Reilly, and E. M. Peterson, *Phys. Rev. B* **1**, 1953 (1970).

¹⁰M. Beck and H. Granicher, *Helv. Phys. Acta* **23**, 522 (1950).

¹¹S. G. P. Brosnan and D. T. Edmonds, *Phys. Lett. A* **81**, 243 (1981).

¹²M. Chabin and F. Gilletta, *Ferroelectrics* **15**, 149 (1977).